Phase Transitions of the Polariton Condensate in 2D Dirac Materials

Ki Hoon Lee,[1,2] Changhee Lee,[2] Hongki Min,[2,*] and Suk Bum Chung[1,2,3,†]
[1]Center for Correlated Electron Systems, Institute for Basic Science (IBS), Seoul National University, Seoul 08826, Korea
[2]Department of Physics and Astronomy, Seoul National University, Seoul 08826, Korea
[3]Department of Physics, University of Seoul, Seoul 02504, Korea

(Received 1 October 2017; published 9 April 2018)

For the quantum well in an optical microcavity, the interplay of the Coulomb interaction and the electron-photon (e-ph) coupling can lead to the hybridizations of the exciton and the cavity photon known as polaritons, which can form the Bose-Einstein condensate above a threshold density. Additional physics due to the nontrivial Berry phase comes into play when the quantum well consists of the gapped two-dimensional Dirac material such as the transition metal dichalcogenide MoS_2 or WSe_2. Specifically, in forming the polariton, the e-ph coupling from the optical selection rule due to the Berry phase can compete against the Coulomb electron-electron (e-e) interaction. We find that this competition gives rise to a rich phase diagram for the polariton condensate involving both topological and symmetry breaking phase transitions, with the former giving rise to the quantum anomalous Hall and the quantum spin Hall phases.

DOI: 10.1103/PhysRevLett.120.157601

Monolayers of transition metal dichalcogenide (TMDC), such as MoS_2 and WSe_2, have attracted widespread interest in recent years as a semiconductor analogue of graphene. Like graphene, they are atomically thin, 2D materials, whose band extrema occurring at the Brillouin zone corners K and K' can be described very well by the Dirac Hamiltonian, that gives rise to the $\pm\pi$-Berry phase at each valley, but, unlike graphene, possess direct band gaps at K and K' [1].

Given the band structure origin of the valley Berry phase, we may ask whether and how it may be affected by the e-e interaction and the e-ph coupling. The e-e interaction in TMDC has been observed to give rise to both the e-e pairs, i.e., the Cooper pairs [2], and the electron-hole pairs, i.e., the excitons [3,4], with superconductivity, which arises from the condensation of the former, shown to be possibly topologically nontrivial [2,5,6]. Meanwhile, the optical valley selection rule for the circularly polarized light [1,7,8] shows the strong effect that the π-Berry phase has on the e-ph coupling with direct band gaps ($\sim$1.5 to 2 eV) lying within the visible spectrum [9,10].

The above considerations motivate us to study the condensation of polaritons, emergent bosons from hybridizations of cavity photons and excitons. It is tunable by both the Coulomb e-e interaction and the e-ph coupling for the exciton binding and the photon-exciton hybridization, respectively. Recent years have seen reports in various systems of possible observation of this condensation [11–13] with progress underway for TMDC [14,15]. The room temperature polariton condensation is a possibility, light-matter coupling giving a very small polariton mass [16]. When the polariton lifetime, though limited by the finite lifetimes of both cavity photons and excitons, is much longer than the thermalization time, substantial evidence of superfluidity, such as vortex formation [17], Goldstone modes [18], and the Landau critical velocity [19], has been observed.

In this Letter, we develop a mean-field theory for exciton polaritons in gapped Dirac materials such as TMDCs, and demonstrate that due to the effect of the π-Berry phase, the mean-field electronic band structure with the polariton condensate can undergo symmetry-breaking or topological phase transitions [20] driven by the competition between the e-e interaction and the e-ph coupling that can be tuned by the excitation density. We first apply our mean-field theory to the single valley model to show how the phase transitions arise and then extend the calculation on the physical two valley model to obtain various phases and their topological invariants.

The polariton condensation in our gapped Dirac materials should be derived from the electrons with the Coulomb interaction coupled to coherent photons. Hence, the Hamiltonian we consider would be

$$\begin{aligned}
\hat{H} &= \hat{H}_0 + \hat{H}_{e\text{-}e} + \hat{H}_{\text{ph}} + \hat{H}_{e\text{-ph}} - \mu_X \hat{N}_{\text{tot}}, \\
\hat{H}_0 &= \sum_{\tau=\pm}\sum_{\mathbf{k}} \begin{bmatrix} \hat{c}^\dagger_{\tau,1,\mathbf{k}} & \hat{c}^\dagger_{\tau,2,\mathbf{k}} \end{bmatrix} \mathbf{d}^{(0)}_\tau(\mathbf{k}) \cdot \boldsymbol{\sigma} \begin{bmatrix} \hat{c}_{\tau,1,\mathbf{k}} \\ \hat{c}_{\tau,2,\mathbf{k}} \end{bmatrix}, \\
\hat{H}_{\text{ph}} &= \hbar\omega_c \sum_I \left(\hat{a}^\dagger_I \hat{a}_I + \frac{1}{2} \right), \\
\hat{H}_{e\text{-ph}} &= -\frac{1}{c}\hat{\mathbf{A}} \cdot \sum_{\tau=\pm}\sum_{\mathbf{k}}\sum_{i,j} \mathbf{J}^\tau_{ij}(\mathbf{k}) \hat{c}^\dagger_{\tau,i,\mathbf{k}} \hat{c}_{\tau,j,\mathbf{k}}, \\
\hat{H}_{e\text{-}e} &= \frac{1}{2S}\sum_{\tau,\tau'}\sum_{\mathbf{k}_1,\mathbf{k}_2,\mathbf{q}}\sum_{i,j} V(q) \hat{c}^\dagger_{\tau,i,\mathbf{k}_1-\mathbf{q}} \hat{c}^\dagger_{\tau',j,\mathbf{k}_2+\mathbf{q}} \hat{c}_{\tau',j,\mathbf{k}_2} \hat{c}_{\tau,i,\mathbf{k}_1},
\end{aligned} \tag{1}$$

where $\boldsymbol{\sigma}$ represent the Pauli matrices, I the photon polarization index, $\mathbf{d}_\tau^{(0)}(\mathbf{k}) \equiv (\tau\hbar v k_x, \hbar v k_y, E_{\rm gap}/2)$, with $\tau = \pm$ being the valley index, ω_c the cavity photon frequency, and $V(\mathbf{q}) = (2\pi e^2/\epsilon q)$ the Coulomb interaction, with ϵ being the dielectric constant; note that the exchange terms of the e-e interaction are in the orbital rather than the band basis [22–24]. Meanwhile, the first quantized current operator is given by $\mathbf{J}_{ij}^\tau(\mathbf{k}) = -\frac{e}{\hbar}\partial_{\mathbf{k}}[\mathbf{d}_\tau^{(0)}(\mathbf{k})\cdot\boldsymbol{\sigma}]_{ij}$ $(i,\ j = 1,\ 2)$ and the gauge field operator by $\hat{\mathbf{A}} = \sum_I \sqrt{2\pi c^2\hbar/\epsilon S L_c \omega_c}(\mathbf{e}_I \hat{a}_I e^{-i\omega_c t} + \mathbf{e}_I^* \hat{a}_I^\dagger e^{i\omega_c t})$, where $\mathbf{e}_I$ is the photon polarization vector and S, L_c the cavity area and length, respectively. $\hat{c}_{1(2)}$ and $\hat{a}_I$ are the annihilation operators for the electron in the $L_z = 0$ $(L_z = 2\tau)$ orbital and the photon with the polarization I, respectively. Each valley is taken to be completely spin polarized with opposite spin polarization, i.e., $S_z = \tau/2$, due to the transition metal atomic spin-orbit coupling $\mathbf{L}\cdot\mathbf{S}$ removing the spin degeneracy in the $L_z = 2\tau$ orbital; hence, the dark excitons from the intravalley spin flip [25] will not be considered. Lastly, $\hat{N}_{\rm tot} = \sum_I \hat{a}_I^\dagger \hat{a}_I + \hat{N}_{\rm ex}$ is the total number of excitations, both photons and excitons, in the system and tuned by the chemical potential μ_X. Since the number of exciton $\hat{N}_{\rm ex}$ is the number of electrons excited from the valence band to the conduction band, the band basis for the electrons, $\sum_\alpha [W(\mathbf{k})]_{i,\alpha}\hat{\psi}_{\alpha,\mathbf{k}} = \hat{c}_{i,\mathbf{k}}$ which diagonalizes $\hat{H}_0$ of Eq. (1) with $\hat{\psi}_{c(v)}$ as the annihilation operator of electrons in the conduction (valence) band, can be convenient. This allows us to identify the exciton number as $\hat{N}_{\rm ex} \equiv \sum_{\tau,\mathbf{k}} \hat{n}_{{\rm ex},\mathbf{k}}^\tau$ where $\hat{n}_{{\rm ex},\mathbf{k}}^\tau \equiv (\hat{\psi}_{\tau,c,\mathbf{k}}^\dagger \hat{\psi}_{\tau,c,\mathbf{k}} + \hat{\psi}_{\tau,v,\mathbf{k}}\hat{\psi}_{\tau,v,\mathbf{k}}^\dagger)/2$. Physically, we are interested in the thermal quasiequilibrium that is reached after the cooling of a population of hot polaritons initially introduced by a short laser pulse [26]. For simplicity, we shall set the temperature to be zero.

We use the BCS variational wave function for the polariton condensate [23,24]

$$|\Psi\{\Lambda_\pm\}\rangle = \mathcal{N}\prod_{I,\tau=\pm,\mathbf{k}} e^{\Lambda_I \hat{a}_I^\dagger}(u_{\tau,\mathbf{k}} + v_{\tau,\mathbf{k}}\hat{\psi}_{\tau,c,\mathbf{k}}^\dagger \hat{\psi}_{\tau,v,\mathbf{k}})|0\rangle \quad (2)$$

with $\mathcal{N} = e^{-\sum_{I=\pm}\Lambda_I^2/2}$ and $|u_{\tau,\mathbf{k}}|^2 + |v_{\tau,\mathbf{k}}|^2 = 1$, where $I = \pm$ corresponds to the right (left)-handed circular polarization $\mathbf{e}_\pm = (1, \pm i)/\sqrt{2}$, and $|0\rangle$ is the ground state of $\hat{H}_0$, in which photons are absent and all the valence (conduction) band states are occupied (vacant). In this wave function, the photon component gives the coherent state with the number of photons $\langle \hat{a}_I^\dagger \hat{a}_I\rangle = \Lambda_I^2$ and of excitons $\langle \hat{N}_{\tau,{\rm ex}}\rangle = \sum_{\mathbf{k}} |v_{\tau,\mathbf{k}}|^2$; only the excitons with zero center-of-mass momentum are condensed, and the condensation energy arises only from the stronger intravalley—but not from the weaker intervalley—e-e interaction. To determine $\Lambda_\pm, u_{\tau,\mathbf{k}}, v_{\tau,\mathbf{k}}$ that minimize $\langle\Psi\{\Lambda_\pm\}|\hat{H}|\Psi\{\Lambda_\pm\}\rangle$, we obtain the mean-field self-consistency condition not only for the e-e interaction through $\hat{H}_{e\text{-}e}^{\rm MF} = \sum_{\tau,i,j,\mathbf{k}} \tilde{\Delta}_{\tau;ij}(\mathbf{k})\hat{c}_{\tau,i,\mathbf{k}}^\dagger \hat{c}_{\tau,j,\mathbf{k}}$ where [27]

$$\tilde{\Delta}_{\tau;ij}(\mathbf{k}) = -(1/S)\sum_{\mathbf{p}} V(\mathbf{k}-\mathbf{p})\left\langle \hat{c}_{\tau,j,\mathbf{p}}^\dagger \hat{c}_{\tau,i,\mathbf{p}}\right\rangle\Big|_{\mu_X=0,\Lambda_\tau=0}^{\mu_X,\Lambda_\tau}, \quad (3)$$

but also for $\hat{H}_{\rm ph} + \hat{H}_{e\text{-ph}}$, by which Λ_I's are determined as [24]

$$\Lambda_I = -\frac{1}{\hbar\omega_c - \mu_X}\frac{1}{\sqrt{S}}\sum_{\tau,\mathbf{k}} (g_{\mathbf{k}}^{I,\tau})^* \langle \hat{\psi}_{\tau,v,\mathbf{k}}^\dagger \hat{\psi}_{\tau,c,\mathbf{k}}\rangle, \quad (4)$$

using the rotating wave approximation $\hat{H}_{e\text{-ph}} = (1/\sqrt{S})\sum_{\mathbf{k},I,\tau} g_{\mathbf{k}}^{I,\tau}\hat{a}_I \hat{\psi}_{\tau,c,\mathbf{k}}^\dagger \hat{\psi}_{\tau,v,\mathbf{k}} + {\rm H.c.}$ on the e-ph coupling, where $g_{\mathbf{k}}^{I,\tau} = \sqrt{\hbar^3/2\omega_c\epsilon S L_c}\langle c|\mathbf{e}_I\cdot\mathbf{J}^{(\tau)}(\mathbf{k})|v\rangle$ is the e-ph coupling strength, and I the photon circular polarization index. The optical valley selection rule [1] gives us the s-wave e-ph coupling, i.e., $g_{\mathbf{k}}^{I,\tau} = g_0\delta_{I,\tau} + O(k^2)$.

From the self-consistency conditions of Eqs. (3) and (4), we find that there exists the competition between the e-e interaction and the e-ph coupling in the polariton condensation in the Dirac material. We first note that the e-ph coupling induces only the s-wave excitons at both valleys, as Λ_I in Eq. (4) is maximized when the e-ph coupling $g_{\mathbf{k}}^{I,\tau}$ and the exciton correlation $\langle \hat{\psi}_{\tau,c,\mathbf{k}}^\dagger \hat{\psi}_{\tau,v,\mathbf{k}}\rangle$ are in the same symmetry. On the other hand, the e-e interaction may not favor the s-wave exciton when we examine $\hat{H}_{e\text{-}e}^{\rm MF} = \sum_{\tau,\alpha,\beta,\mathbf{k}} \Delta_{\tau;\beta\alpha}(\mathbf{k})\hat{\psi}_{\tau,\beta,\mathbf{k}}^\dagger \hat{\psi}_{\tau,\alpha,\mathbf{k}}$, given that

$$\Delta_{\tau;c,v}(\mathbf{k}) = \sum_{i,j}[W\tilde{\Delta}W^\dagger]_{\tau;c,v}(\mathbf{k}) \approx \Delta_{\tau;c,v}^s(k) + e^{i\tau\phi_{\mathbf{k}}}\Delta_{\tau;c,v}^p(k),$$

$$\Delta_{\tau;c,v}^s(k) \approx -\frac{1}{S}\cos^2\frac{\theta_k}{2}\sum_{\mathbf{p}} V(|\mathbf{k}-\mathbf{p}|)\langle \hat{\psi}_{\tau,v,\mathbf{p}}^\dagger \hat{\psi}_{\tau,c,\mathbf{p}}\rangle\cos^2\frac{\theta_p}{2},$$

$$\Delta_{\tau;c,v}^p(k) \approx \frac{1}{S}\sin\theta_k\sum_{\mathbf{p}} V(|\mathbf{k}-\mathbf{p}|)\langle \hat{n}_{{\rm ex},\mathbf{p}}^\tau\rangle\cos\theta_p, \quad (5)$$

where $\tan\phi_{\mathbf{k}} \equiv k_y/k_x$, $\tan\theta_k \equiv \hbar v k/(E_{\rm gap}/2)$. The p-wave components $\Delta_{\tau;c,v}^p(k)$ arise from the $\tau\pi$ Berry phase, as can be seen both from the chiralities of the p-wave components for the two valleys being opposite and $\Delta_{\tau;c,v}^p(k)$ being proportional to $\sin\theta_k$, the integrated Berry curvature of $\hat{H}_0$ for momenta smaller than k, that vanishes linearly as $k \to 0$. We see from Eq. (5) that the Coulomb e-e interaction favors the p-wave (s-wave) exciton at the τ valley when the τ-valley exciton density $\sum_{\mathbf{p}}\langle \hat{n}_{{\rm ex},\mathbf{p}}^\tau\rangle$ becomes sufficiently large (small) compared to the critical density set by the average Berry curvature. We will show that when the exciton symmetry of the polariton condensate is predominantly chiral p wave in the τ valley, the Berry phase sign of τ valley changes in the mean-field Hamiltonian $\hat{H}^{\rm MF} \equiv \hat{H}_0 + \frac{1}{\sqrt{S}}\sum_{I,\tau,\mathbf{k}}(\Lambda_I g_{\mathbf{k}}^{I,\tau}\hat{\psi}_{\tau,c,\mathbf{k}}^\dagger \hat{\psi}_{\tau,v,\mathbf{k}} + {\rm H.c.}) + \hat{H}_{e\text{-}e}^{\rm MF} - \mu_X\hat{N}_{\rm ex}$ from

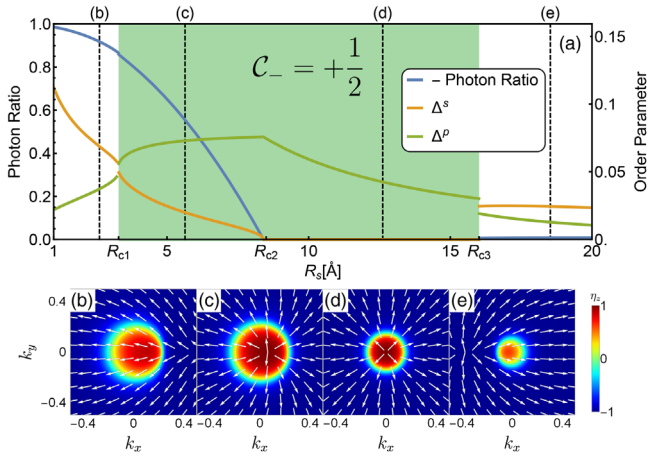

FIG. 1. (a) Photon fraction and mean-field band exciton gap parameters $\Delta^{s,p}$ averaged over the momentum space as the functions of R_s for the photon frequency $\hbar\omega_c = 2.1$ eV, the dielectric constant $\epsilon = 10$, the Dirac velocity $\hbar v = 3.7$ eV Å, and the band gap of $E_{\rm gap} = 2.0$ eV. (b)–(e) Pseudospin textures at the R_s values indicated in (a). Arrow represents $\hat{\boldsymbol{\eta}}_\parallel$ and false color represents $\eta_z(\mathbf{k})$; for convenience, we have plotted the $\tau = -$ valley coupled to $I = -$ photons.

that of $\hat{H}_0$. While Eq. (5) also indicates that the chiral p-wave excitons are due to a component of the e-e interaction that violates the $N_{\rm tot}$ conservation [28], the $N_{\rm tot}$ fluctuation remains small, i.e., $[\langle(\Delta\hat{N}_{\rm tot})^2\rangle/N_{\rm tot}^2] = \{[\Lambda^2+\sum_{\mathbf{k}}|u_{\mathbf{k}}|^2|v_{\mathbf{k}}|^2]/[(\Lambda^2+\sum_{\mathbf{k}}|v_{\mathbf{k}}|^2)^2]\} \ll 1$.

The essence of the competition between the e-e interaction and the e-ph coupling can emerge clearly from considering only a single valley, i.e., the $\tau = -$ valley coupled to the $I = -$ photons, revealing how the competition can give rise to the phase transition of our polariton condensate. Figure 1(a) shows how the photon fraction $\Lambda^2/(\Lambda^2 + \langle\hat{N}_{\rm ex}\rangle)$ of the polariton condensate and the exciton gap parameters $\Delta^{s,p}$ of Eq. (5) depend on the mean distance $R_s \equiv \sqrt{S/N_{\rm tot}\pi}$ between excitations, the quantity that determines the total number of excitations $N_{\rm tot}$. A key feature here is that the p-wave excitons are dark [29], which can be confirmed from Λ vanishing in Eq. (4) for the purely p wave $\langle\hat{\psi}_v^\dagger\hat{\psi}_c\rangle$ because of the s-wave symmetry for the e-ph coupling, i.e., $g_{\mathbf{k}} \approx g_0\delta_{I,\tau}$. Since Δ^p arises solely from the e-e interaction, the higher-density discontinuous crossing of $|\Delta^s|$ and $|\Delta^p|$ curves in Fig. 1(a) at $R_s = R_{c1}$ can be regarded as a consequence of the competition between the e-e interaction and the e-ph coupling.

The lower density transition in Fig. 1(a) at $R_s = R_{c3}$ involves little e-ph coupling, and can be attributed to the competition between different components of the e-e interactions shown in Eq. (5), which favors the chiral p-wave exciton for the large $\sum_{\mathbf{k}}\langle\hat{n}^\tau_{{\rm ex},\mathbf{k}}\rangle$ (or small R_s) and the s-wave exciton for the small $\sum_{\mathbf{k}}\langle\hat{n}^\tau_{{\rm ex},\mathbf{k}}\rangle$ (or large R_s). As shown in Figs. 1(b)–1(e), the transitions at both $R_s = R_{c1}$ and $R_s = R_{c3}$ can be illustrated using the pseudospin texture defined from the parametrization of the mean-field Hamiltonian: $\sum_{\mathbf{k},\alpha,\beta}\hat{\psi}^\dagger_{\alpha,\mathbf{k}}[\boldsymbol{\sigma}\cdot\boldsymbol{\eta}(\mathbf{k})]_{\alpha\beta}\hat{\psi}_{\beta,\mathbf{k}} \equiv \hat{H}^{\rm MF}$. One can see that both transitions involve the (dis)appearance of the skyrmion texture in the $\hat{\boldsymbol{\eta}}$ configuration, which requires in the $\eta_z > 0$ region the singularity of $\hat{\boldsymbol{\eta}}_\parallel \equiv \hat{\boldsymbol{\eta}} - (\hat{\boldsymbol{\eta}}\cdot\hat{\mathbf{z}})\hat{\mathbf{z}}$, while $\hat{\boldsymbol{\eta}} = -\hat{z}$ as $k \to \infty$. However, Figs. 1(d) and 1(e) show that, for the $R_s = R_{c3}$ transition, the $\hat{\boldsymbol{\eta}}_\parallel$ singularity jumps from $\mathbf{k} = 0$ to the $\eta_z < 0$ region, while for the $R_s = R_{c1}$ transition, the $\hat{\boldsymbol{\eta}}_\parallel$ singularity jumps from the $\eta_z < 0$ region into the $\eta_z \gtrsim 0$ region away from $\mathbf{k} = 0$, nearly closing the quasiparticle energy gap. This implies that the topological phase transition at $R_s = R_{c3}$ also involves the changes in the exciton symmetry.

Overall, the Fig. 1 plots show how the topological phase transition of $\hat{H}^{\rm MF}$ can arise from the competition between the s-wave and the chiral p-wave exciton pairing channels. The Chern number of a single valley can be defined in a manner analogous to that of the topological insulator surface [30], with the understanding that the integer value is obtained when summed with that of the other valley. Note how the Chern number $\mathcal{C}_- = \pm\frac{1}{2}$ coincides exactly with $|\Delta^s| < |\Delta^p|$ ($|\Delta^s| > |\Delta^p|$) in Fig. 1(a). $\mathcal{C}_-$ can be computed equivalently in either the orbital basis obtained from $\boldsymbol{\sigma}\cdot\hat{\mathbf{d}} = W(\sigma\cdot\hat{\boldsymbol{\eta}})W^\dagger$ or the band basis as $\mathcal{C}_- = (1/4\pi)\int d^2k\hat{\mathbf{d}}\cdot(\partial_{k_x}\hat{\mathbf{d}}\times\partial_{k_y}\hat{\mathbf{d}}) = -\frac{1}{2} + (1/4\pi)\int d^2k\hat{\boldsymbol{\eta}}\cdot(\partial_{k_x}\hat{\boldsymbol{\eta}}\times\partial_{k_y}\hat{\boldsymbol{\eta}})$, which is consistent with Figs. 1(b)–1(e) as it gives $\mathcal{C}_- = \pm\frac{1}{2}$ when the skyrmion is present (absent); note that $\hat{H}_0$ gives $\mathcal{C}_- = -\frac{1}{2}$. In fact, we may define the overall exciton symmetry to be a chiral p wave when $\mathcal{C}_- = +\frac{1}{2}$. Given that the Δ^p arises from the nonconservation of $N_{\rm tot}$ as can be seen from Eq. (5), this is a case of discontinuous phase transitions to excitonic insulator phases in the absence of the $N_{\rm tot}$ conservation, though our case deals with quantum rather than the classical phase transitions considered in Refs. [31,32].

The full phase diagrams with respect to R_s and the photon detuning $\delta \equiv \hbar\omega_c - E_{\rm gap}$ shown as Fig. 2 for different values of the dielectric constant ϵ and the band gap $E_{\rm gap}$ can be largely explained by the different energy competitions that give rise to the higher and the lower density phase transition. δ and ϵ are control parameters in the competition between the e-ph coupling and the e-e interaction; the photon self-consistency equation Eq. (4) shows that the smaller δ leads to the larger photon fraction, while the smaller ϵ leads to the larger e-e interaction. Figure 2(b) shows that the $\mathcal{C}_- = +\frac{1}{2}$ phase with the chiral p-wave excitons requires sufficiently weak e-ph coupling, which is naturally larger for the smaller Coulomb interaction of $\epsilon = 15$ shown in red than for the larger Coulomb interaction of $\epsilon = 10$ shown in blue and green. That the lower density (larger R_s) transition depends little on δ confirms its weak dependence on the e-ph coupling. Meanwhile, the blue curves of Fig. 2(b) show that for a

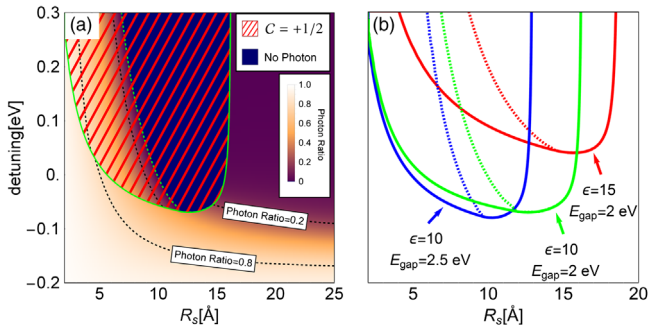

FIG. 2. (a) The dependence of photon fraction for the single-valley TMDC polariton system on δ and R_s shown with $\hbar v = 3.7$ eV Å, $\epsilon = 10$ and $E_{\rm gap} = 2.0$ eV; the green solid, the green dashed and the black dotted curves represent the first-order transitions, the second-order transitions, and the crossovers, respectively. (b) Phase boundaries for the first-order (solid) and second-order (dashed) transitions for $\epsilon = 10$ and $E_{\rm gap} = 2$ eV (green), $\epsilon = 15$ and $E_{\rm gap} = 2$ eV (red), and $\epsilon = 10$ and $E_{\rm gap} = 2.5$ eV (blue).

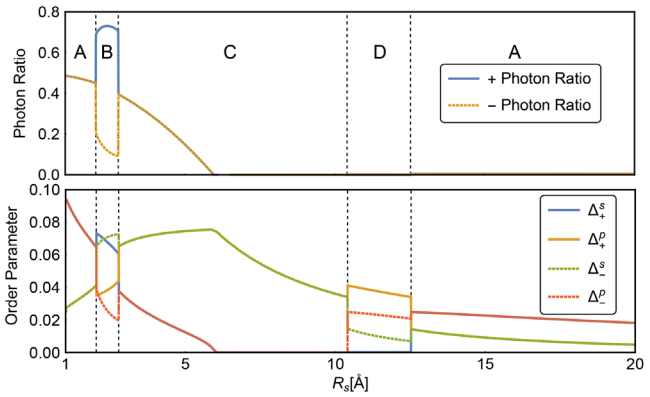

FIG. 3. Photon fraction (above) and mean-field band exciton gap parameters $\Delta^{s,p}$ (below) for two valleys ($\tau = \pm 1$) as the functions of R_s for the photon frequency $\hbar\omega_c = 2.1$ eV and other physical parameters following those of Fig. 2(a).

larger $E_{\rm gap}$ the lower density transition occurs at smaller R_s (larger density) when compared with the lower $E_{\rm gap}$ shown by the green and red curves. This is because of the larger $E_{\rm gap}$ suppressing Δ^p through reducing $\sin\theta_k$ at all momenta, or, equivalently, the Berry curvature integrated over momenta smaller than k.

The phase diagram of Fig. 2(a) shows phase transitions as well as crossovers in contrast to the results for the polariton condensate in the topologically trivial quantum well where only the latter were present [23]. Following the results of Kamide *et al.* for the topologically trivial quantum well, we can define in the $\mathcal{C}_- = -\frac{1}{2}$ region several phases according to the photon fraction as the photon, the polariton, and the exciton BEC in decreasing order, with their boundaries being crossovers (shown as the dotted curves). However, as discussed above, there is a first-order phase transition (shown as the solid curves) between the $\mathcal{C}_- = -\frac{1}{2}$ and the $\mathcal{C}_- = +\frac{1}{2}$ regions. Within the $\mathcal{C}_- = +\frac{1}{2}$ region, the phase with the vanishing photon fraction would be best termed the electron-hole BCS condensate, R_s being smaller than the p-wave exciton radius [33]. Inside the $\mathcal{C}_- = +\frac{1}{2}$ region, there is a second-order phase transition (shown as the dashed curves) between the polariton BEC and this electron-hole BCS condensate involving the spontaneous rotational symmetry breaking. Despite photons providing no preferred direction, the rotational symmetry is broken when we have both the s-wave and the chiral p-wave components in $v_{\mathbf{k}}/u_{\mathbf{k}}$ of the exciton wave function Eq. (2), which moves the singularity of $\boldsymbol{\eta}_{\parallel}$ textures of Figs. 1(b), 1(c), and 1(e) away from $\mathbf{k} = 0$. The rotational symmetry in our polariton condensate is restored in Fig. 1(d) on Λ and Δ^s vanishing continuously. Hence, our polariton condensate is always distinct from the $\hat{H}_0$ ground state in either topology or symmetry.

For the two valley TMDCs coupled to photons of both circular polarizations shown in Fig. 3, we find that the topological phase transitions give rise to both the quantum spin Hall phase (in the region C) and the quantum anomalous Hall phase (in the regions B and D). To analyze this problem, we consider the variational solution of Eq. (2) with the phase difference between the two photon polarizations fixed. In the absence of interactions, $\hat{H}_0$ of Eq. (1) gives us the opposite sign for the Chern numbers of $\mathcal{C}_\tau = (\tau/2)$ for the τ valley. When the exciton symmetry of one valley is the chiral p wave and that of the other valley is the s wave, we have a net Chern number of $\mathcal{C}_{\rm tot} \equiv \sum_{\tau,\sigma}\mathcal{C}_{\tau,\sigma} = \pm 1$ for our $\hat{H}^{\rm MF}$ and hence the quantum anomalous Hall phase [35]. Because of the valley polarization that occurs only in this phase, the regions B and D have the elliptic photon polarizations while all the other regions have the linear photon polarizations. Meanwhile, the region C of Fig. 3 shows that the photon fraction and the Δ^s at both valleys vanish continuously at the same R_s [36]. In the region C, we have the quantum spin Hall phase where the time-reversal symmetry is restored by the opposite chirality between the p-wave excitons of the two valleys. Table I shows the topological phases for the two-valley TMDC

TABLE I. Phase classification in the two valleys coupled to the photons of both circular polarizations. The alphabet letters in the leftmost column refer to each phase mentioned in Fig. 3. $\mathcal{C}_S \equiv \sum_{\tau,\sigma}\sigma\mathcal{C}_{\tau,\sigma}/2$ and $\mathcal{C}_V \equiv \sum_{\tau,\sigma}\tau\mathcal{C}_{\tau,\sigma}/2$ are the spin and the valley Chern numbers, respectively. Refer the main text for further details.

	$\mathcal{C}_{+\uparrow}$	$\mathcal{C}_{+\downarrow}$	$\mathcal{C}_{-\uparrow}$	$\mathcal{C}_{-\downarrow}$	$\mathcal{C}_S$	$\mathcal{C}_V$	$\mathcal{C}_{\rm tot}$
A	$+1/2$	$+1/2$	$-1/2$	$-1/2$	0	$+1$	0
B	$\pm 1/2$	$+1/2$	$-1/2$	$\pm 1/2$	$-1/2$	$+1/2$	± 1
C	$-1/2$	$+1/2$	$-1/2$	$+1/2$	-1	0	0
D	$\mp 1/2$	$+1/2$	$-1/2$	$\mp 1/2$	$-1/2$	$+1/2$	∓ 1

polariton condensate taking into account both spin components at each valley.

In summary, we found topological phase transitions in the quasiequilibrium ground state of the TMDC monolayer coupled to the cavity photons due to the competition between the e-ph coupling and the e-e interaction tuned by the excitation density. Our approach is expected to work best for the thermal quasiequilibration time shorter than the polariton lifetime. We may find the regions of our phase diagram with optimal experimental accessibility as the quasiequilibration time may depend on various physical parameters, e.g., R_s. One possible method for triggering our phase transitions may be the terahertz pump which has been shown to induce the s-wave to p-wave transition in the excitons [37].

We would like to thank Xi Dai, Hans Hansson, Joon Ik Jang, Na Young Kim, S. Raghu, Yao Wang, and Fengcheng Wu for sharing their insights. S. B. C. acknowledges the hospitality of Nordita during its conference on "Multi-Component and Strongly Correlated Superconductors" where parts of this work have been completed. This research was supported by IBS-R009-Y1 (K. H. L. and S. B. C.) and Basic Science Research Program through the National Research Foundation of Korea (NRF) funded by the Ministry of Education under Grant No. 2015R1D1A1A01058071 (C. L. and H. M.).

*hmin@snu.ac.kr
†sbchung0@uos.ac.kr

[1] D. Xiao, G.-B. Liu, W. Feng, X. Xu, and W. Yao, Coupled Spin and Valley Physics in Monolayers of MoS_2 and Other Group-VI Dichalcogenides, Phys. Rev. Lett. **108**, 196802 (2012).
[2] J. M. Lu, O. Zheliuk, I. Leermakers, N. F. Q. Yuan, U. Zeitler, K. T. Law, and J. T. Ye, Evidence for two-dimensional ising superconductivity in gated MoS_2, Science **350**, 1353 (2015).
[3] D. Y. Qiu, F. H. da Jornada, and S. G. Louie, Optical Spectrum of MoS_2: Many-Body Effects and Diversity of Exciton States, Phys. Rev. Lett. **111**, 216805 (2013).
[4] M. M. Ugeda, A. J. Bradley, S.-F. Shi, F. H. da Jornada, Y. Zhang, D. Y. Qiu, W. Ruan, S.-K. Mo, Z. Hussain, Z.-X. Shen, F. Wang, S. G. Louie, and M. F. Crommie, Giant bandgap renormalization and excitonic effects in a monolayer transition metal dichalcogenide semiconductor, Nat. Mater. **13**, 1091 (2014).
[5] N. F. Q. Yuan, K. F. Mak, and K. T. Law, Possible Topological Superconducting Phases of MoS_2, Phys. Rev. Lett. **113**, 097001 (2014).
[6] Y.-T. Hsu, A. Vaezi, M. H. Fischer, and E.-A. Kim, Topological superconductivity in monolayer transition metal dichalcogenides, Nat. Commun. **8**, 14985 (2017).
[7] T. Cao, G. Wang, W. Han, H. Ye, C. Zhu, J. Shi, Q. Niu, P. Tan, E. Wang, B. Liu, and J. Feng, Valley-selective circular dichroism of monolayer molybdenum disulphide, Nat. Commun. **3**, 887 (2012).
[8] H. Zeng, J. Dai, W. Yao, D. Xiao, and X. Cui, Valley polarization in MoS_2 monolayers by optical pumping, Nat. Nanotechnol. **7**, 490 (2012).
[9] K. F. Mak, C. Lee, J. Hone, J. Shan, and T. F. Heinz, Atomically Thin MoS_2: A New Direct-Gap Semiconductor, Phys. Rev. Lett. **105**, 136805 (2010).
[10] A. Splendiani, L. Sun, Y. Zhang, T. Li, J. Kim, C.-Y. Chim, G. Galli, and F. Wang, Emerging photoluminescence in monolayer MoS_2, Nano Lett. **10**, 1271 (2010).
[11] H. Deng, G. Weihs, C. Santori, J. Bloch, and Y. Yamamoto, Condensation of semiconductor microcavity exciton polaritons, Science **298**, 199 (2002).
[12] J. Kasprzak, M. Richard, S. Kundermann, A. Baas, P. Jeambrun, J. M. J. Keeling, F. M. Marchetti, M. H. Szymańska, R. André, J. L. Staehli, V. Savona, P. B. Littlewood, B. Deveaud, and L. S. Dang, Bose–Einstein condensation of exciton polaritons, Nature (London) **443**, 409 (2006).
[13] R. Balili, V. Hartwell, D. Snoke, L. Pfeiffer, and K. West, Bose-einstein condensation of microcavity polaritons in a trap, Science **316**, 1007 (2007).
[14] X. Liu, T. Galfsky, Z. Sun, F. Xia, E.-c. Lin, Y.-H. Lee, S. Kéna-Cohen, and V. M. Menon, Strong light–matter coupling in two-dimensional atomic crystals, Nat. Photonics **9**, 30 (2015).
[15] Y.-J. Chen, J. D. Cain, T. K. Stanev, V. P. Dravid, and N. P. Stern, Valley-polarized exciton–polaritons in a monolayer semiconductor, Nat. Photonics **11**, 431 (2017).
[16] J. J. Baumberg, A. V. Kavokin, S. Christopoulos, A. J. D. Grundy, R. Butté, G. Christmann, D. D. Solnyshkov, G. Malpuech, G. Baldassarri Höger von Högersthal, E. Feltin, J.-F. Carlin, and N. Grandjean, Spontaneous Polarization Buildup in a Room-Temperature Polariton Laser, Phys. Rev. Lett. **101**, 136409 (2008).
[17] K. G. Lagoudakis, M. Wouters, M. Richard, A. Baas, I. Carusotto, R. Andre, L. S. Dang, and B. Deveaud-Pledran, Quantized vortices in an exciton-polariton condensate, Nat. Phys. **4**, 706 (2008).
[18] S. Utsunomiya, L. Tian, G. Roumpos, C. W. Lai, N. Kumada, T. Fujisawa, M. Kuwata-Gonokami, A. Loffler, S. Hofling, A. Forchel, and Y. Yamamoto, Observation of bogoliubov excitations in exciton-polariton condensates, Nat. Phys. **4**, 700 (2008).
[19] A. Amo, J. Lefrere, S. Pigeon, C. Adrados, C. Ciuti, I. Carusotto, R. Houdre, E. Giacobino, and A. Bramati, Superfluidity of polaritons in semiconductor microcavities, Nat. Phys. **5**, 805 (2009).
[20] By contrast, previous studies, e.g., Ref. [21], dealt with the topology of the effective polariton bands.
[21] T. Karzig, C.-E. Bardyn, N. H. Lindner, and G. Refael, Topological Polaritons, Phys. Rev. X **5**, 031001 (2015).
[22] F. M. Marchetti, J. Keeling, M. H. Szymańska, and P. B. Littlewood, Thermodynamics and Excitations of Condensed Polaritons in Disordered Microcavities, Phys. Rev. Lett. **96**, 066405 (2006).
[23] K. Kamide and T. Ogawa, What Determines the Wave Function of Electron-Hole Pairs in Polariton Condensates?, Phys. Rev. Lett. **105**, 056401 (2010).
[24] T. Byrnes, T. Horikiri, N. Ishida, and Y. Yamamoto, BCS Wave-Function Approach to the BEC-BCS Crossover of

Exciton-Polariton Condensates, Phys. Rev. Lett. **105**, 186402 (2010).

[25] J. P. Echeverry, B. Urbaszek, T. Amand, X. Marie, and I. C. Gerber, Splitting between bright and dark excitons in transition metal dichalcogenide monolayers, Phys. Rev. B **93**, 121107 (2016).

[26] T. Byrnes, N. Y. Kim, and Y. Yamamoto, Exciton-polariton condensates, Nat. Phys. **10**, 803 (2014).

[27] The no-photon ground state value in the Fock potential is subtracted off so that $\hat{c}_{\mathbf{k}}$'s can be treated as the non-interacting quasiparticles with our band parameters.

[28] See Supplemental Material at http://link.aps.org/supplemental/10.1103/PhysRevLett.120.157601 for details of the model, the mean-field approximation, and the angular decomposition.

[29] Z. Ye, T. Cao, K. O'Brien, H. Zhu, X. Yin, Y. Wang, S. G. Louie, and X. Zhang, Probing excitonic dark states in single-layer tungsten disulphide, Nature (London) **513**, 214 (2014).

[30] X.-L. Qi, T. L. Hughes, and S.-C. Zhang, Topological field theory of time-reversal invariant insulators, Phys. Rev. B **78**, 195424 (2008).

[31] L. Keldysh and Y. V. Kopaev, Possible instability of semimetallic state toward coulomb interaction, Sov. Phys. Solid State **6**, 2219 (1965).

[32] M. J. Rice and S. Strässler, Theory of the soft phonon mode and dielectric constant below the Peierls transition temperature, Solid State Commun. **13**, 1931 (1973).

[33] Following Ref. [34], with the dielectric constant of $\epsilon = 10$ and the band gap of $E_{\mathrm{gap}} = 2.0$ eV, we obtain the exciton radius of $a_{\mathrm{ex}}^{(s)} = 5.2$ Å for the s wave and $a_{\mathrm{ex}}^{(p)} = 46$ Å for the p wave.

[34] X. L. Yang, S. H. Guo, F. T. Chan, K. W. Wong, and W. Y. Ching, Analytic solution of a two-dimensional hydrogen atom. I. Nonrelativistic theory, Phys. Rev. A **43**, 1186 (1991).

[35] F. D. M. Haldane, Model for a Quantum Hall Effect Without Landau Levels: Condensed-Matter Realization of the "Parity Anomaly", Phys. Rev. Lett. **61**, 2015 (1988).

[36] The rotational symmetry breaking at two valleys is not independent due to the e-ph coupling. Therefore, if we take the $\hat{H}_0$ of Eq. (1), i.e., with the continuous rotational symmetry, we have for the two valley case the SO(2) rather than $\mathrm{SO}(2) \times \mathrm{SO}(2)$ symmetry breaking. Given the photon polarization, the vanishing photon fraction is necessary for the rotational symmetry.

[37] J. M. Ménard, C. Poellmann, M. Porer, U. Leierseder, E. Galopin, A. Lemaître, A. Amo, J. Bloch, and R. Huber, Revealing the dark side of a bright exciton–polariton condensate, Nat. Commun. **5**, 4648 (2014).